$O(N)$ real-space method for *ab initio* quantum transport calculations: Application to carbon nanotube–metal contacts

Marco Buongiorno Nardelli,[1] J.-L. Fattebert,[1,2] and J. Bernholc[1]
[1]*Department of Physics, North Carolina State University, Raleigh, North Carolina 27695-8202*
[2]*Center for Applied Scientific Computing, Lawrence Livermore National Laboratory, California 94551*
(Received 8 May 2001; published 10 December 2001)

We present an *ab initio* $O(N)$ method that combines an accurate optimized-orbital solution of the electronic structure problem with an efficient Green's function technique for evaluating the quantum conductance. As an important illustrative example, we investigate carbon nanotube–metal contacts and explain the anomalously large contact resistance observed in nanotube devices as due to the spatial separation of their conductance eigenchannels. The results for various contact geometries and strategies for improving device performance are discussed.

DOI: 10.1103/PhysRevB.64.245423 PACS number(s): 72.80.Rj, 73.61.Wp, 73.40.−c

I. INTRODUCTION

The study of the electrical properties of nanostructures has seen intense activity in the last decade, due to the promise of novel technological applications for nanoscale quantum electronic devices. The theoretical study of quantum conductance in such structures has thus become of primary interest and has been addressed by a variety of techniques.[1] Due to the complexity of describing an ''open'' system of a nanoscale device in contact with effectively infinite leads, most of the current approaches rely on phenomenological tight binding models, which for many systems may not provide a sufficiently reliable and accurate description.

There are only few examples of *ab initio* calculations of quantum conductance and the field is still in a critical phase of development. The existing methods are based on the solution of the quantum scattering problem for the electronic wave functions through the conductor using a number of related techniques: Lippman-Schwinger and perturbative Green's function methods have been used to study conductance in metallic nanowires and recently in small molecular nanocontacts;[2,3] conduction in nanowires, junctions, and nanotube systems has been addressed using local[4] or nonlocal[5,6] pseudopotential methods and through the solution of the coupled-channel equations in a scattering-theoretic approach.[7–9] These methods are based on a plane wave representation of the electronic wave functions, which imposes severe restrictions on the size of the system because of the large number of basis functions necessary for an accurate description of the electron transmission process. Therefore, structureless jellium leads, which do not provide a microscopic description of the conductor-metal contact, had to be assumed in most cases for computational reasons. Only recently have real-space approaches been considered for a more efficient solution of the electronic transport problem. They are based on the use of linear combination of atomic orbitals[10] (LCAO) or Gaussian[11] orbital bases. These are combined with either a scattering state solution for the transmission[10] or Green's function–based techniques.[11]

In this paper we present an approach based on a real-space optimized-orbital solution of the electronic structure problem, combined with an efficient Green's function–based technique for the evaluation of the electron transmission probability. Both the *ab initio* and the transport algorithms scale essentially linearly with the size of the system, thus extending greatly the range of applicability of our method. This method has been already successfully applied to describe quantum conductance in ideal and defective carbon nanotubes.[12] Following a brief overview of the methodology, we address the problem of contacts in a metal-carbon nanotube assembly, which is very important in the design of efficient nanotube-based devices. Contact resistances of the order of MΩ are typically observed in most of the prototypical nanotube-based devices realized so far,[13–16] whereas from simple band structure arguments one would expect resistances of the order of a few tenths of kΩ,[17] because the fundamental resistance of a single ballistic channel is 12.9 kΩ. The results of our calculations provide an explanation for this pathologically high contact resistance and suggest strategies to improve the performance of nanotube-metal contacts. It is important to stress that this problem requires self-consistent *ab initio* methodology, in order to accurately describe the highly inhomogeneous environment of a nanowire-metal junction and to account for the charge transfer occurring at the interface between the two dissimilar materials.

II. METHODOLOGY

Our *ab initio* calculations of quantum conductance utilize an expansion of the Hamiltonian, the Green's functions, and related quantities in a basis of localized orbitals.[18] It is then possible to efficiently evaluate the quantum conductance of a lead-conductor-lead system in $O(N)$ steps, by dividing the system into principal layers that interact only with their nearest neighbors. In order to perform the *ab initio* electronic structure calculation, we use a real-space, optimized-orbital method that attains essentially linear scaling by utilizing atom-centered localized functions, while optimizing their shape.[19] Real-space grids are used throughout, which allows for straightforward application of localization constraints and for multigrid convergence acceleration on all length scales. The variational optimization of the orbitals leads to high ac-

curacy while using only a minimal basis (see below). The relatively low cost of the method allows for *ab initio* treatment of the infinite leads in full atomistic detail, and for a complete and consistent description of the coupling of the conductor with the leads.

The conductance G of the full open system (infinite left lead, conductor, infinite right lead) is evaluated via the transmission function as[1,20,21]

$$G=\frac{2e^2}{h}\mathcal{T}=\frac{2e^2}{h}\mathrm{Tr}\,(\Gamma_L G_C \Gamma_R G_C), \tag{1}$$

where G_C is Green's function of the conductor (C) and $\Gamma_{\{L,R\}}$ are functions that describe the coupling of the conductor to the left (L) and right (R) leads. Equation (1) is valid in both the Landauer approach and in the noninteracting limit of the Keldysh nonequilibrium Green's function formulation.[21] In a general nonorthogonal localized orbital scheme, the Green's function of the whole system can be explicitly written as[1]

$$G_C=(\epsilon\mathcal{S}_C-H_C-\Sigma_L-\Sigma_R)^{-1}, \tag{2}$$

where Σ_L and Σ_R are the self-energy terms due to the semi-infinite leads, and H_C and S_C are the Hamiltonian and overlap matrices for the localized orbitals in the conductor. The coupling functions $\Gamma_{\{L,R\}}$ can be easily obtained once the self-energy functions are known:[1,18,22,23]

$$\Gamma_{\{L,R\}}=i[\Sigma^r_{\{L,R\}}-\Sigma^a_{\{L,R\}}].$$

The expression of the self-energies can be deduced along the lines of Ref. 18 using the formalism of principal layers in the framework of the surface Green's function-matching theory.[22] We obtain

$$\begin{aligned}\Sigma_L&=(\epsilon\mathcal{S}_{LC}-H_{LC})^{\dagger}[\epsilon\mathcal{S}^L_{00}-H^L_{00}+(\epsilon\mathcal{S}^L_{01}-H^L_{01})^{\dagger}\overline{T}_L]^{-1}\\&\quad\times(\epsilon\mathcal{S}_{LC}-H_{LC}),\\ \Sigma_R&=(\epsilon\mathcal{S}_{CR}-H_{CR})[\epsilon\mathcal{S}^R_{00}-H^R_{00}+(\epsilon\mathcal{S}^R_{01}-H^R_{01})T_R]^{-1}\\&\quad\times(\epsilon\mathcal{S}_{CR}-H_{CR})^{\dagger},\end{aligned} \tag{3}$$

where $H^{L,R}_{nm}$ are the matrix elements of the Hamiltonian between layer orbitals of the left and right leads, respectively. $\mathcal{S}^{L,R}_{nm}$ are the corresponding overlap matrices and $T_{L,R}$ and $\overline{T}_{L,R}$ are the appropriate transfer matrices. The latter are easily computed from the Hamiltonian and overlap matrix elements via an iterative procedure.[18,23] Correspondingly, H_{LC}, H_{CR}, S_{LC}, and S_{CR} are the coupling and overlap matrices for the conductor-lead assembly.

The procedure above requires the knowledge of the Hamiltonian and overlap matrix elements between layer orbitals of the left and right leads, together with the matrix elements describing the coupling in the conductor-lead assembly. To compute these matrices,[24] *ab initio* density-functional calculations are carried out using the $O(N)$-like algorithm described in Ref. 19. Briefly, given an atomic configuration and the corresponding Kohn-Sham Hamiltonian

$$H=-\frac{1}{2}\nabla^2+V_{\mathrm{ion}}+V_H(\rho)+\mu_{\mathrm{xc}}(\rho), \tag{4}$$

where V_{ion}, V_H, and μ_{xc} represent the ionic pseudopotentials, the Hartree potential, and the exchange-correlation potential, respectively, we minimize the total energy functional

$$\begin{aligned}E[\{\phi_i\}_{i=1}^N]&=2\,\mathrm{Tr}(H^{(\phi)}\overline{\rho}^{(\phi)})-\frac{1}{2}\int\frac{\rho(\mathbf{r})\rho(\mathbf{r}')}{|\mathbf{r}-\mathbf{r}'|}d\mathbf{r}\,d\mathbf{r}'\\&\quad-\int\mu_{\mathrm{xc}}(\rho)\rho(\mathbf{r})d\mathbf{r}+E_{\mathrm{xc}}[\rho]\end{aligned} \tag{5}$$

for a set of nonorthogonal orbitals $\{\phi_i\}_{i=1}^N$. Here $\overline{\rho}^{(\phi)}$ is the density matrix in the basis $\{\phi\}$. The electronic density is then given by

$$\rho(\mathbf{r})=2\sum_{j,k=1}^{N}(\overline{\rho}^{(\phi)})_{jk}\phi_j(\mathbf{r})\phi_k(\mathbf{r}). \tag{6}$$

The $N\times N$ matrix $H^{(\phi)}$ is defined by $H^{(\phi)}_{ij}=\langle\phi_i|H|\phi_j\rangle$. We also define the overlap matrix $S^{(\phi)}_{ij}=\langle\phi_i|\phi_j\rangle$.

The calculations use numerical orbitals defined on a uniform grid in real space. They are centered on atoms and localized in spherical regions of radius R_L around the respective atoms. The orbitals are variationally optimized using multigrid preconditioning techniques until they accurately describe the ground state of the system. This procedure allows us to use a small number of orbitals per atom, much smaller than in LCAO or Gaussian-based calculations, because the orbitals are optimized on the grid according to their environment. The size of the matrices that enter in the quantum conductance calculation and the computational cost of the whole procedure are thus minimized. In order to ensure fast convergence and accuracy—even for metallic systems—we use both occupied and unoccupied orbitals. The scaling of the most expensive parts of the calculations is still $O(N)$ due to localization, but there is a small $O(N^3)$ part, which is dealt with by effective parallelization.[19]

The matrices that enter in the electronic transport calculation are computed in two steps. In the first calculation, we compute the ground state of the bare leads in a supercell with periodic boundary conditions. From this calculation we extract the real-space Hamiltonian and overlap matrices required for the computation of the self-energy operators. We then perform a second calculation in a supercell containing the conductor and one principal layer of the leads. In this calculation, the orbitals in the leads are kept the same as in the bare lead calculation, in order to extract the matrix elements and overlaps needed in the definition of the conductor region and to describe the coupling between the conductor and the leads. This procedure accounts fully for the electronic structure of the conductor and the interaction between the conductor and the leads, provided that the lead region is large enough to avoid spurious interactions between periodic images of the contacts. In order to have interactions between the nearest-neighbor principal layers only, the width of the layers has to be sufficiently large compared to the localization regions. On the other hand, the localization regions have

to be large enough to ensure an accurate solution of the density-functional equations. Moreover, in the Green's function–matching procedure one has to carefully align the Fermi levels of both systems in order to avoid spurious bias effects. (In this paper we will limit the discussion to the linear response regime and thus to zero bias across the conductor-lead junctions.) Provided that in the conductor-lead calculation the lead region is large enough to recover bulklike behavior far from the interfaces, we align the macroscopic average of the electrostatic potentials in the bare lead and in the conductor-lead geometry. This ensures a seamless conductor-lead geometry and prevents the spurious bias. An equivalent procedure is often used to extract band offsets in superlattice calculations.[25,26]

III. RESULTS

The methodology above has been used to study electronic transport in carbon nanotube–metal contacts. The metal contacts are modeled as Al crystals oriented in the [111] direction. A (5,5) carbon nanotube (diameter ≈ 7 Å) is deposited on a metal surface, establishing an electrical contact on one side. In both the bare-lead and lead-nanotube calculations the simulation cells were chosen large enough (14.7 and 29.5 Å, respectively) to be consistent with a relatively large localization radius ($R_L \approx 5$ Å) for the orbitals, needed for an accurate description of the metallic system. We use two optimized orbitals per Al atom, and three per C atom. The total numbers of atoms in the two simulation cells are 220 and 340, respectively,. These configurations have been extensively tested to ensure full convergence of the electronic structure. A grid spacing of 0.18 Å, corresponding to a 45 Ry cutoff, is employed throughout. We use the local density exchange-correlation functional and Hamann nonlocal pseudopotentials.[27] All atomic geometries are fully relaxed. The resulting equilibrium distance between the nanotube and the Al surface is 3.4 Å and we observe an outward relaxation of the (111) Al surface of $\approx 1.6\%$, in agreement with other local-density calculations.[28] The interaction between the two systems is quite weak (90 meV/atom), and no major relaxation/reconstruction of the nanotube-metal complex is observed. Moreover, the choice of relatively long contact regions in the bare lead geometry ensures a minimal lattice mismatch between the nanotube and the Al surface. Given the weak interaction between the two, a small ($\approx 1\%$) residual mismatch does not affect the electronic or transport properties of the system.

Turning to the results, we first discuss an ideal, infinitely long nanotube deposited on a metal surface. The geometry considered here is shown in the inset of the left panel of Fig. 1. The main characteristic of the electronic response is a marked charge transfer from the nanotube to the metal that allows the valence band edge of the nanotube to align with the Fermi level of the metal electrode.[29] This charge transfer, which has already been observed for other systems in experiments[13,31,15] and calculations,[29,30,39] leads to enhanced conductivity along the tube axis and gives rise to a weak ionic bonding between the tube and the metal. The conductance spectrum for the nanotube is displayed in the left panel

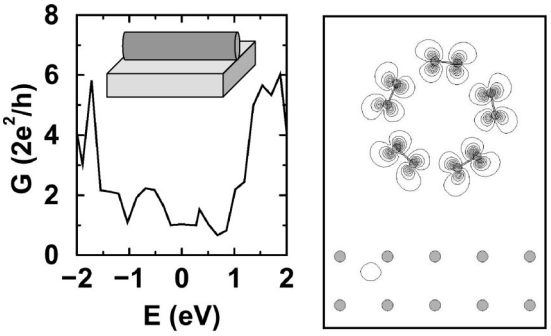

FIG. 1. Left panel: The geometry and conductance spectrum of an infinite (5,5) nanotube deposited on Al(111). Right panel: cross section of the probability density of the electronic wave function corresponding to the only open eigenchannel at the Fermi level that has a sizable component on the nanotube. The other wave functions at the Fermi level are mostly localized on the metal.

of Fig. 1, in units of $2e^2/h$. The main effect observable in the spectrum is the short plateau around the Fermi level with unit conductance. This is at variance with the ideal value of two, which comes from the two electron bands of an isolated armchair nanotube that are available for transmission. Although the metal contact increases the resistance by a factor of 2 when compared to the ideal, isolated nanotube, it appears that a sizable degree of electron transmission through the system should still occur.

In order to better understand the contrast between these results and the anomalously high resistance observed in experiments,[13,15,16] we analyze the total conductance in terms of *eigenchannels* for the transmission,[32] by exploiting the localized orbital structure of our method to separate the individual (nanotube and metal) contributions to conductance. The transmission eigenchannels are defined as the eigenvectors $\{\mathbf{U}\}$ that diagonalize the transmission matrix in Eq. (1) in the Landauer-Buttiker form:[33]

$$\mathbf{U}\mathcal{T}\,\mathbf{U}^{\dagger} = \mathbf{U}\mathbf{t}\mathbf{t}^{\dagger}\mathbf{U}^{\dagger} = \mathrm{diag}\{\tau_i\}, \tag{7}$$

where $\mathbf{t}$ is the left-to-right transmission amplitude matrix and τ_i are the eigenchannel transmissions.[34] The eigenchannels form a complete orthonormal basis of the subspace spanned by the localized orbitals of the conductor. They have well-defined transmissions, i.e., without interchannel scattering, and their characteristics give direct information about the properties of the transmission process.

Among the conducting channels (those with nonvanishing transmission τ_i), we observe a clear distinction between eigenchannels mainly localized in the metal region and those on the nanotube. This result reflects the separation between individual electronic wave functions of the system.

In particular, the eigenchannel corresponding to the plateau of conductance around the Fermi energy corresponds to an individual wave function, reproduced in the right panel of Fig. 1, that is almost fully localized on the nanotube (93%). This implies that there is very little hybridization and intermixing between the nanotube and the metal in the channel responsible for conduction at the Fermi level. Thus, the conduction electron transfer between the tube and the metal in

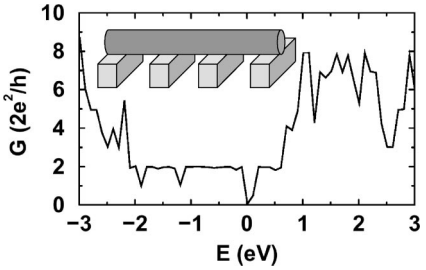

FIG. 2. The conductance spectrum of a periodic array of finite metallic nanocontacts, as shown in the inset. The Fermi level is taken as a reference.

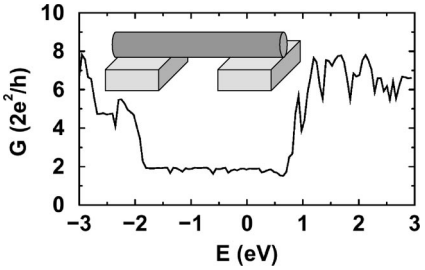

FIG. 3. The conductance spectrum of an ideal two-terminal device shown in the inset. The Fermi level is taken as a reference.

the idealized side-contact geometry considered here is very inefficient, which can explain the pathologically high contact resistance observed in nanotube-metal contacts.[13,15,16] In particular, this example clearly demonstrates that the weak nanotube-metal coupling is mostly responsible for the weak electron transport in the combined system, while wave vector conservation is not a significant factor.[17,35] The weak distributed coupling is also the reason for the measured contact resistance being inversely proportional to contact length.[14,36,37] A conductance of one has also been observed in an experiment that measured electron transfer between a liquid metal and a multiwalled nanotube,[36] but the conditions of this experiment allow for several alternative explanations.[38]

The real-space, principal-layer formalism and the rapid screening of charge disturbances allow us to carry out related calculations with modest additional effort. Using the results of the first calculation, two other contact geometries were considered. The first is a periodic (infinite) array of narrow metallic wires crossing an infinite nanotube, with both contacts and tube bridges being 1.5 nm wide. This configuration and the resulting conductance spectrum are shown in Fig. 2. The main characteristic is an opening of a semiconducting gap in the otherwise almost ideal nanotube spectrum. It is induced by the breaking of the mirror symmetry of the nanotube wave functions induced by the localized perturbation of the nanocontacts. The gap in the electronic band structure at the Fermi energy is clearly reflected in the local density of states computed from the Green's function G_C. A similar result was previously obtained for a copper chain in contact with a nanotube.[39]

Finally, we discuss the contact geometry shown in Fig. 3 (inset). It more closely resembles an experimental two-terminal device, with two semi-infinite contacts connected by a nanotube bridge, 1.5 nm long. In this geometry, the system recovers the ideal conductance of an isolated tube with two conductance channels at the Fermi energy, as shown in Fig. 3. This behavior is induced by the alignment of the valence band edge of the nanotube with the Fermi energy of the metal contacts, triggered by the charge transfer in the lead regions. In this particular geometry, these conditions restore the two original eigenchannels of the nanotube and thus conserve the number of conducting channels throughout the system. It is important to note that the weak nanotube-metal interaction, responsible for the pathologically high resistance of the nanotube-metal assembly, is not strengthened. Both eigenchannels are highly localized on the nanotube, with a negligible fraction on the metal contacts, and closely resemble the channel[40] shown in the right panel of Fig. 1. Although the nanotube behaves as an ideal ballistic conductor, the bonding characteristics of the nanotube-metal system prevent an efficient electron transfer mechanism from the nanotube to the Al contact. Indeed, inducing defects in the contact region, e.g., by localized electron bombardment,[16] would drastically increase the bonding strength of the nanotube-metal assembly and greatly improve the performance of the device. Alternatively, we have found that mechanically pushing the nanotube closer to the Al surface by a small amount (≈ 1 Å, with an energy expense of ≈ 10 meV/atom) more than doubles the transmission efficiency between the metal and the nanotube. The mechanical deformation induces a small inward relaxation of the Al surface in the contact region, facilitating stronger hybridization between the nanotube and the metal contact in the conducting channels and thus contributing to a higher electron transmission rate between the two systems.

IV. SUMMARY

In summary, we have developed an efficient *ab initio* method to compute quantum conductances in nanostructures. As a first application, the transport properties of carbon nanotube–metal contacts were investigated. The calculations provide a clear interpretation of current experimental results for a variety of contact geometries and suggest avenues for improving the properties of nanotube-metal assemblies in potential nanoscale electronic devices, such as rectifiers, actuators, and nanoswitches.

ACKNOWLEDGMENTS

It is a pleasure to thank Dr. Vincent Meunier for many fruitful discussions. This work was supported by ONR, DOE, and NASA. A portion of the work was performed under the auspices of the U.S. Department of Energy by University of California Lawrence Livermore National Laboratory under Contract No. W-7405-Eng-48.

[1] See, for instance, S. Datta, *Electronic Transport in Mesoscopic Systems* (Cambridge University Press, Cambridge, 1995); F. Ferry and S. Goodnick, *Transport in Nanostructures* (Cambridge University Press, Cambridge, 1997).
[2] N. Lang, Phys. Rev. B **52**, 5335 (1995).
[3] M. Di Ventra, S. Pantelides, and N. Lang, Phys. Rev. Lett. **84**, 979 (2000).
[4] J.-L. Mozos *et al.*, Phys. Rev. B **56**, R4351 (1997).
[5] H. Choi and J. Ihm, Phys. Rev. B **59**, 2267 (1999).
[6] H. Choi, J. Ihm, S. Louie, and M. Cohen, Phys. Rev. Lett. **84**, 2917 (2000).
[7] K. Hirose and M. Tsukada, Phys. Rev. B **51**, 5278 (1995).
[8] N. Kobayashi, M. Brandbyge, and M. Tsukada, Phys. Rev. B **62**, 8430 (2000).
[9] U. Landman, R. Barnett, A. G. Scherbakov, and P. Avouris, Phys. Rev. Lett. **85**, 1958 (2000).
[10] Y.-G. Yoon, M. S. C. Mazzoni, H. J. Choi, J. Ihm, and S. G. Louie, Phys. Rev. Lett. **86**, 688 (2001).
[11] S. N. Yaliraki, A. E. Roitberg, C. Gonzalez, V. Mujica, and M. A. Ratner, J. Chem. Phys. **11**, 6997 (1999).
[12] M. Buongiorno Nardelli, J.-L. Fattebert, D. Orlikowski, C. Roland, Q. Zhao, and J. Bernholc, Carbon **38**, 1703 (2000).
[13] S. Tans, R. M. Verschueren, and C. Dekker, Nature (London) **393**, 49 (1998).
[14] S. Tans *et al.*, Nature (London) **386**, 474 (1997).
[15] R. Martel, T. Schmidt, H. Shea, and P. Avouris, Appl. Phys. Lett. **73**, 2447 (1998).
[16] A. Bachtold *et al.*, Appl. Phys. Lett. **73**, 274 (1998).
[17] J. Tersoff, Appl. Phys. Lett. **74**, 2122 (1999).
[18] M. Buongiorno Nardelli, Phys. Rev. B **60**, 7828 (1999); M. Buongiorno Nardelli and J. Bernholc, *ibid.* **60**, R16338 (1999).
[19] J.-L. Fattebert and J. Bernholc, Phys. Rev. B **62**, 1713 (2000).
[20] D. Fisher and P. Lee, Phys. Rev. B **23**, 6851 (1981).
[21] Y. Meir and N. Wingreen, Phys. Rev. Lett. **68**, 2512 (1992).
[22] F. Garcia-Moliner and V. Velasco, Phys. Rep. **200**, 83 (1991); *Theory of Single and Multiple Interfaces* (World Scientific, Singapore, 1992).
[23] M. Lopez-Sancho, J. Lopez-Sancho, and J. Rubio, J. Phys. F: Met. Phys. **14**, 1205 (1984); **15**, 851 (1985).
[24] Although the calculation of the Green's function requires a matrix inversion that scales as $O(N^3)$, the localization of the orbitals allows us to divide the system into smaller subsystems and compute the quantities of interest in largely $O(N)$ fashion [see also, for instance, M. P. Anantram and T. R. Govindan, Phys. Rev. B **58**, 4882 (1998)].
[25] A. Baldereschi, S. Baroni, and R. Resta, Phys. Rev. Lett. **61**, 734 (1988).
[26] M. Buongiorno Nardelli, K. Rapcewicz, and J. Bernholc, Phys. Rev. B **55**, R7323 (1997).
[27] D. R. Hamann, Phys. Rev. B **40**, 2980 (1989).
[28] N. Marzari (private communication).
[29] Y. Xue and S. Datta, Phys. Rev. Lett. **83**, 4844 (1999).
[30] A. Rubio *et al.*, Phys. Rev. Lett. **82**, 3520 (1999).
[31] J. Wildoer *et al.*, Nature (London) **391**, 59 (1998).
[32] M. Brandbyge, M. Sorensen, and K. Jacobsen, Phys. Rev. B **56**, 14 956 (1997).
[33] M. Buttiker, Y. Imri, R. Landauer, and S. Pinhas, Phys. Rev. B **31**, 6207 (1985).
[34] J. C. Cuevas, A. Levy Yeyati, and A. Martin-Rodero, Phys. Rev. Lett. **80**, 1066 (1998).
[35] P. Delaney and M. Di Ventra, Appl. Phys. Lett. **75**, 4028 (1999).
[36] S. Frank, P. Poncharal, Z. Wang, and W. A. de Heer, Science **280**, 1744 (1998).
[37] M. Anantram, S. Datta, and Y. Xue, Phys. Rev. B **61**, 14 219 (2000).
[38] H. J. Choi, J. Ihm, Y. G. Yoon, and S. Louie, Phys. Rev. B **60**, R14 009 (1999); P. Delaney, M. Di Ventra, and S. T. Pantelides, Appl. Phys. Lett. **75**, 3787 (1999); S. Sanvito, Y. K. Kwon, D. J. Tomanek, and C. J. Lambert, Phys. Rev. Lett. **84**, 1974 (2000).
[39] K. Kong, S. Han, and J. Ihm, Phys. Rev. B **60**, 6074 (1999).
[40] Note that the occurrence of a single channel in the former case is due to the idealized geometry of an infinite nanotube on an infinite metallic surface. The conservation of the total number of channels is ensured by the channels localized on the metal.